HEAT TRANSFER STUDIES ON A SIMULATED 600 KW INDUCTION MOTOR

BISWAJIT BANERJEE
Deptt. of Mechanical Engineering,
Assam Engineering College,
Guwahati : 781013.

K. V. CHALAPATHI RAO, V. M. K. SASTRI
Deptt. of Mechanical Engneering,
Indian Institute of Technology,
Madras : 600 036.

ABSTRACT :

Experimental and analytical investigations are carried out for the determination of heat transfer coefficients between corotating and stationary parallel disks with internal heat generation. The experimental model simulates a typical induction motor with unequal losses in the stator and rotor. The data collected cover a range of Reynolds and Taylor numbers for various heat inputs. Quantitative assessment has been made for the increase in heat transfer with speed of rotation and coolant flow, air being the cooling medium. Temperatures along the axial, radial and tangential directions are measured, and heat transfer coefficients at the radially diverging section are evaluated. The disk configuration has been discretised into suitable lumps and a resistance network has been formed, for which the convective resistances have been calculated using the heat transfer coefficients evaluated experimentally. The resistance network has been solved on a digital computer and the predicted value of temperatures at the corresponding nodal points are found to be in good agreement with the measured values.

1. INTRODUCTION :

Prediction of temperature distribution in an electric machine is a subject matter of great interest to researchers and engineers.

Direct measurement of temperature in the rotor winding and core portions is very difficult, expensive and often impossible under service conditions. One has to resort to indirect methods. Electrical analogue approach is one of the most commonly used methods for the prediction of temperature distribution for both steady and unsteady state conditions.

In order to determine the steady or transient temperature distribution using network solutions, It is essential to know the nature of fluid flow in the cooling passages. Depending on whether the flow is laminar or turbulent, suitable heat transfer coefficients are assumed and the convective resistances calculated. These are linked with the conductive resistances and an appropriate network is formed. It appears from the literature that no stgnificant work has been done to determine the heat transfer coefficients in rotating ducts similar to the configuration that exists in typical electric machines. For example, if one considers the stack of laminations (of the stator and rotor bodies) separated by spacers, it will closely resemble two parallel disks transferring heat by axial convection to the air flowing out radially.

Harada [1] made numerical investigations on the flow between two rotating disks using von karman's similarity hypothesis. The analysis was carried out for various angular velocity ratios and did not take heat transfer into account.Several authors [2,3,4] reported work on heat transfer from a disk with or without enclosure and for the case of parallel disks [5] without rotation. Mochizuki and Yang [6] reported work with corotating parallel disks but with steam as the heating fluid. To the authors' knowledge, no

work has so far been reported for the determination of heat transfer coefficient for the case of corotating parallel disks together with concentric stationary parallel disks, a configuration that closely resembles the rotor–stator of an electric machine, with forced or free convection taking place between the disks.

The experimentally obtained heat transfer coefficients for the rotor and stator radial ducts obtained by geometrical simulation of a 600 kw induction motor for a typical heating condition are presented in this paper. The values of these heat transfer coefficients are used to calculate the convective resistances of the two and three dimensional networks constructed for the disk assembly. The temperature distribution obtained by the solution of the networks are compared with those measured experimentally.

2. EXPERIMENTAL SETUP :

The experimental setup simulates the rotor and stator of a typical induction motor. It consists of essentially four pairs of disks forming three radial ducts. Attention is paid to the central duct whereas the remaining two ducts on either side take care of the end effects. A sectional view of the test section is shown in Fig. 1. For simplicity each bunch of laminations of the motor is idealised to be a simple disk of solid steel. The disks are held in position by means of tie rods and end flanges which are suitably insulated to minimise axial coduction. The rotor is fixed to two end flanges fitted to a hollow shaft through which thermocouples and power leads are taken out.

The simulate the heat generation due to copper losses in the conductor, rectangular heater elements are inseted into the slots made in the periphery of the rotor and stator disks. The maximum heating capacity of each of the stator and rotor heaters is 125 W and 80 W respectively. Heat loads to these heating elements are given proportional to the heat losses typical as machine.

The rotor–stator air gap is about 1 mm. Both rotor and stator surfaces are chrome-plated to prevent rust formation and thus maintain a clean surface. A power slipring with brushes is used for power supply to heating elements. Precautions are taken to prevent slipping and short circuiting of the heating elements even at high rotational speeds. A variable speed drive is connected to the rotor shaft through a pulley machanism for varying the speeds.

The coolant used is air and its flow path is shown in Fig. 2. The air required for the test is obtained from a centrifugal blower, and the actual flow rates of the coolant air in the test section range from 1.3×10^{-2} to 2.7×10^{-2} kg/s. The air is uniformly admitted all over the rotor annulus, through the circular openings in the stator and rotor end flanges on the right. Then it enters the radial ducts of the rotor and finally comes out at the back of the stator disks. The exhaust air is let off to the atmosphere.

The disk faces are numbered R1, R2....., S1. S2..... for easy location of the thermocouples (Fig. 2). Numbers of double-insulated copper–constantan thermocouples are fixed at different locations (Figs. 3 and 4) on the disk surfaces. The rotor thermocouples are brought out through the hollow shaft and finally connected to a slipring mechanism. The output of the slipring mechanism is given to a selector switch and a digital voltmeter whereas the stator thermocouples are connected directly to the selector switch. The slipring mechanism is gold plated and has negligible contact drop and capable of working at speeds upto 15,000 rpm. Temperatures in the axial, tangential and radial directions are measured to and accuracy of 0.1^{0} C . Experiments are carried for various Taylor and Reynolds numbers.

3. NETWORK FORMULATION :

The main principle of the electrical analogy method is the replacement of the thermal resistance circuits by the equivalent electrical ones, using lumped system analysis as there exists an analogy between heat flow and flow of electricity.

The governing differential equation for one dimensional heat flow in a conductor is,

$$\frac{\delta^2 T}{\delta x_t^2} = \frac{1}{\alpha} \frac{\delta T}{\delta \gamma_t} \quad \cdots\cdots (1)$$

and unidirectional current flow in an electrical conductor is governed by.

$$\frac{\delta^2 V}{\delta x_e^2} = RC \frac{\delta v}{\delta \gamma_e} \quad \cdots\cdots (2)$$

From a close study of equations (1) and (2) it can be inferred that

Temperature is analogous to voltage,

Heat flow is analogous to current flow,

Thermal resistance is analogous to electrical resistance,

Thermal capacity is analogous to electrical capacitance, and

Thermal time is analogous to electrical time.

The thermal problem can, therefore, be transformed into an electrical one by the following procedure. The thermal quantities are expressed in a consistent system of units, the thermal system is divided into volume elements which are replaced by equivalent electrical elements. Each electrical element is to possess the same number of units of resistance and capacitance as the corresponding thermal element. Thus the values of voltage rise and current at a given time and at a given point in the circuit correspond numerically to the values of temperature rise and heat flow at that time and position in the thermal system. Similarly a three dimensional thermal problem may be replaced by an electrical circuit in which each element in the thermal arrangement is represented by a single capacitance and three resistors. By proper inclusion of the terms in the equation, the convective resistances can also be represented in the form of electrical resistances in the electrical network.

Using the above method, two and three dimensional networks are constructed for the two pairs of disks on either side of the central duct, as shown in Figs. 5 and 6 respectively. Heat inputs in the thermal system are represented as current sources in the electrical networks. The nodes in the networks correspond to the nodes as marked on the disk surfaces (Fig. 3 &4). However, the stator part of the network has two additional nodes along radial direction, one each at the extreme radial positions.

4. RESULTS AND DISCUSSION :

Experiments are carried out for the following operating conditions : Re = 1825–3850 for the rotor and a corresponding Re = 1150–2450 for the stator. The correspondence of the rotor and stator Reynolds numbers is based on the same mass flow rate of air. Speed of rotation of the rotor is varied from 0 to 700 r. p. m., which corresponds to a Taylor number range 0–102. Of the various stator/rotor heat inputs experimented, observations for a 600/300 W combination are reported here.

The heat transfer coefficient is defined on the basis of logarithmic mean temperature difference, assuming fully developed flow for most of the passage length :

$$h = Q \ln \frac{(T_{w,out}-T_{c,out})/(T_{w,in}-T_{c,in})}{A\,(T_{w,out}-T_{c,out})-(T_{w,in}-T_{c,in})} \quad ..(3)$$

Where $T_{w,in} = (T_{10}+T_{14}+T_5+T_1+)/4$ for stator (Fig.3)

$= (T_8+T_6+T_1+T_3)/4$ for rotor (Fig.4)

$T_{w,out} = (T_{13}+T_{17}+T_8+T_4)/4$ fot stator (Fig.3)

$= (T_9+T_7+T_2+T_4)/4$ for rotor (Fig.4)

$T_{w,in}$ and $T_{w,out}$ are measured on the disk wall surfaces at the same radial location as $T_{c,in}$ and $T_{c,out}$, respectively. The location of thermocouples for measurement of air temperatures $T_{c,in}$ and $T_{c,out}$ are indicated in Fig.2.

The Taylor number (Ta), based on disk spacing, is defined as :

Ta= $\beta^2 \Omega / \nu$..... .....(4)

The heat transfer performance is expressed in terms of the Nusselt number, and plots are made against Re and Ta for the given heat input. For heat transfer calculations, all the physical properties of air are evaluated at the arithmetic mean of the temperatures of air at the inlet and exit of the core.

The Nusselt number is defined in terms of the disk spacing as :-

$Nu = h\, D_H / k$..... (5)

Figures 7 and 8 show the variation of Nu plotted against Re for various Taylor numbers, for both the rotor and the stator. Although the stator is not rotating Fig. 8 indicates the influence of the

rotation of the rotor on the stator heat transfer augmentation. It is seen from Fig. 7 that the Nusselt number for the rotor radial duct increases monotonically with increase in Re. The value of Nu at the upper limit of Re is almost double its value at the lower limit of Re, for the range of Re considered. Whereas Fig. 8 indicates considerable increase in stator heat transfer with increase in Re, the effect appears to reach a maximum at the maximum Re investigated. However, experimentation at still higher Reynolds numbers are required to cofirm this trend.

In order to find the Nusselt number for no-flow condition (Re=0) for different Taylor numbers, the graphs, when extended to intercept the ordinate (Fig. 9 and 10) show good agreement with a work carried out earlier for no-flow conditions (7), thus establishing the reliability of the present investigation.

The temperature predictions from the 3–D and 2–D network analogue for the disk assembly are compared with the experimentally measured values in Tables 1 and 2, for the minimum and maximum Re, at various Taylor numbers. The percentage overprediction or underprediction of the analogue results with respect to the experimental are also shown in the tables. As mentioned earlier, because of lack of any suitable correlation for the heat transfer coefficients for the rotor–stator configuration, the experimentally obtained heat transfer coefficients have been used as inputs into both 3–D and 2–D analogues for temperature predictions.

It is observed that the 3–D predictions for the stator differ from the measured values in the range of –2.5 to 12%, at the lower Re and from 4.5 to 13.5% at the higher Re. Similary, for the rotor, the variations are from 11 to 16% at the lower Re and from –0.5 to 15% at the higher Re.

The difference between the 2–D predictions and the measured values for the stator is from –12 to 6.5% at the lower Re and from 5.5%to 19% at the higher Re, the corresponding differences for the rotor being 0.4% to 20% and from –2% to 21.5%

TABLE 1

Comparison of Analogue Temperatures with Experimentel Results
(Nodes prefixed S refer to stator and prefixed R refer to rotor as shown in Figs. 3 & 4 respectively)
Stator/Rotor heat input : 600/300 W
Stator/Rotor Re : 1150/1825

Ta	Nodes	Exptl. Temp.°C (1)	3-D Analog. Temp.°C (2)	2-D Analog. Temp.°C (3)	% Difference (1)-(2) / (1)	% Difference (1)-(3) / (1)
	S1	55.2	55.9	58.8	1.26	6.52
	S2	54.9	55.2	56.7	0.54	3.27
0	S3	54.6	54.8	54.3	0.36	-0.55
	S4	54.4	53.7	50.6	-1.28	-6.98
	R1	45.2	50.9	49.5	12.61	9.51
	R2	47.4	53.0	55.4	11.81	16.87
	S1	54.0	55.9	57.2	3.65	5.92
	S2	53.5	55.2	56.4	3.23	5.42
44	S3	53.2	53.8	54.5	12.40	2.44
	S4	53.0	52.9	52.1	-0.18	-1.69
	R1	41.9	47.8	48.6	14.17	15.99
	R2	43.1	50.0	52.5	16.08	21.81
	S1	53.0	54.3	56.3	2.47	6.22
	S2	52.5	53.6	55.4	2.06	5.52
73	S3	52.1	52.2	52.8	0.21	1.34
	S4	51.9	51.4	50.6	-1.06	-2.50
	R1	40.4	46.5	48.1	15.22	19.06
	R2	41.5	47.7	49.3	15.06	18.79
	S1	50.7	52.0	52.2	2.50	2.85
	S2	50.5	51.5	50.4	2.08	-0.19
102	S3	50.5	49.9	46.3	-1.16	-8.30
	S4	50.3	49.0	44.2	-2.46	-12.12
	R1	39.3	45.8	47.7	11.34	21.37
	R2	39.9	45.9	42.0	14.97	5.13

TABLE 2

Stator/Rotor heat input : 600/300 W
Stator/Rotor Re : 2450/3850

Ta	Nodes	Exptl. Temp.°C (1)	3-D Analog. Temp.°C (2)	2-D Analog. Temp °C (3)	% Difference (1)-(2)/(1)	% Difference (1)-(3)/(1)
	S1	43.4	48.8	51.6	12.53	18.89
	S2	42.8	48.0	50.8	12.26	18.83
0	S3	42.4	46.7	47.3	10.21	11.58
	S4	42.0	45.8	45.4	9.12	8.04
	R1	36.8	40.1	43.5	9.10	18.34
	R2	37.6	42.3	37.4	-0.53	22.13
	S1	42.2	46.5	50.2	10.19	18.95
	S2	41.9	45.8	48.6	9.33	16.11
44	S3	41.9	44.5	46.6	6.08	11.26
	S4	41.7	43.6	44.3	4.48	6.23
	R1	34.6	37.4	39.4	8.03	13.81
	R2	35.7	39.5	36.8	10.64	3.20
	S1	41.1	45.0	48.4	9.53	17.66
	S2	40.6	43.9	47.1	8.15	16.05
73	S3	40.4	42.7	45.2	5.59	11.90
	S4	40.0	41.9	42.8	4.62	7.05
	R1	34.1	36.7	37.2	7.43	13.81
	R2	34.3	37.3	35.4	8.93	10.64
	S1	39.6	44.9	47.4	13.46	19.69
	S2	39.0	44.2	45.6	13.38	17.00
102	S3	38.5	42.9	42.1	11.37	9.48
	S4	38.1	42.0	40.3	10.26	5.69
	R1	33.2	36.4	42.2	9.73	27.08
	R2	33.4	38.5	36.2	15.18	8.38

5. CONCLUSIONS

Using the actual heat transfer coefficient values. instead of any predictions from correlations, appears to be suitable approach to validate the analogue per se.

It can be observed that, in general the 3-D predictions are closer to the experimental values as far as the stator is concerned. However, for the rotor, in some cases the 2-D predictions are in better agreement with experimental values. Thus generally, the 2-D predictions are seen to be more conservative from the design point of view.

6. NOMENCLATURE

A	Heat transfer area $[=(2\pi N/4)(D_2^2 - D_1^2) + \pi NL(D_2 + D_1)]$, m^2
A_c	Area of flow of air $(= \pi D_m B)$, m^2
B	Spacing between disks, m
C	Capacitance : thermal, W s/^oC, electrical, Farad.
D	Disk diameter, m
D_1	Inner diameter, m
D_2	Outer diameter, m
D_H	Hydraulic diameter (=2B), m
D_m	Mean diameter, m
G	Mass velocity $(=m/A_c)$, kg/(m^2 s)
h	Average heat transfer coefficient, W/(m^2 K)
k	Thermal conductivity of air, W/(m K)
L	Axial dimension of the disks, m
m	Mass flow rate of air, kg/s
N	Number of disks
Nu	Nusselt number $(=h D_H/k)$
n	Rotational speed of rotor, rps
Q	Heat input, W
R	Resistance ; thermal, ^{o}C/W; electrical, ohm
Re	Reynolds number $(= GD_H/\mu)$
T	Temperature, ^{o}C
Ta	Taylor number
V	Voltage, Volts
x	Distance, m
α	Thermal diffusivity, m^2/s
Ω	Angular velocity rotor
ϑ	Kinematic viscosity of air, m^2/s
μ	Dynamic viscosity of air, Kg/m.s
γ	Time, sec

7. SUBSCRIPTS

C	Cold fluid
e	Electrical
R	Rotor
S	Stator
t	Thermal
w	Wall

8. REFERENCES

1. Harada, I, On Three Kinds of Solutions of a Flow Between Two Rotating Disks, J. phys. Soc. Japan, Vol.45, 1978,pp 721–722.
2. Sabba Rao, B. K, Heat Transfer from partially Enclosed Disks Rotating in Air, with Uniform Wall Heat Flux, Indian Journal of Technology, Vol.15, 1977,pp 177-184.
3. Soo, S.L., Flow over and Enclosed Rotating Disk, Trans, ASME, Vol. 80, 1958, pp 287–296
4. Mitchell, J.W, and Metzger, D. E, Heat Transfer from a Shrouded Rotating Disk to a Single Fluid Stream, Trans, ASME, Journal of Heat Transfer, Vol.87, 1965,pp 485–492.
5. Mochizuki, S, Yang, W.J, Yagi Y, and Ueno, M, Heat Transfer Machanisms and performance in Multiple parallel Disk Assemblies, Trans. ASME, J. Heat Transfer, Vol.105.105,1983,pp 598-604
6. Mochizuki, S., and Yang, W.J., Heat Transfer and Friction Loss in Laminar Radial Flows through Rotating Annular Disks Trans. ASME, J. Heat Transfer, Vol. 103,1981,pp 212–217,
7. Banerjee, B, Rao, K.V.C, and Sastri V.M.K, Transient Free Convective Heat Transfer from Corotating Concentric Disks, Accepted for publication in International Journal of Heat Mass Transfer.

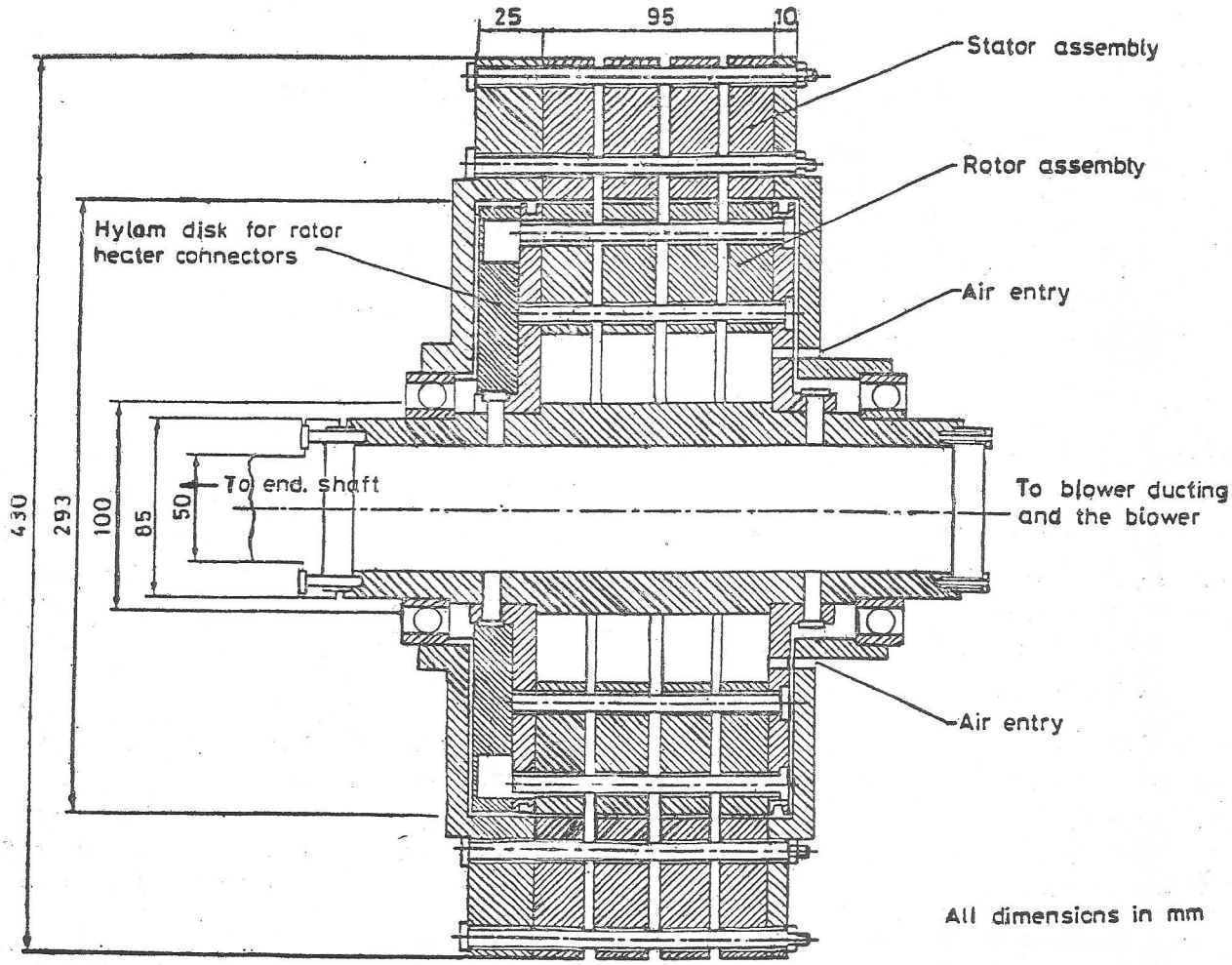

FIG. 1. Sectional view of the test section.

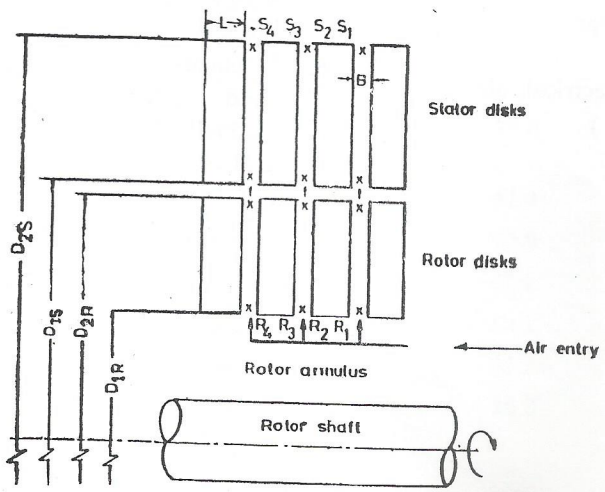

FIG. 2. Numbering of stator & rotor disks for thermocouple locations.

x indicates air thermocouple locations.
arrows indicate the air flow path.

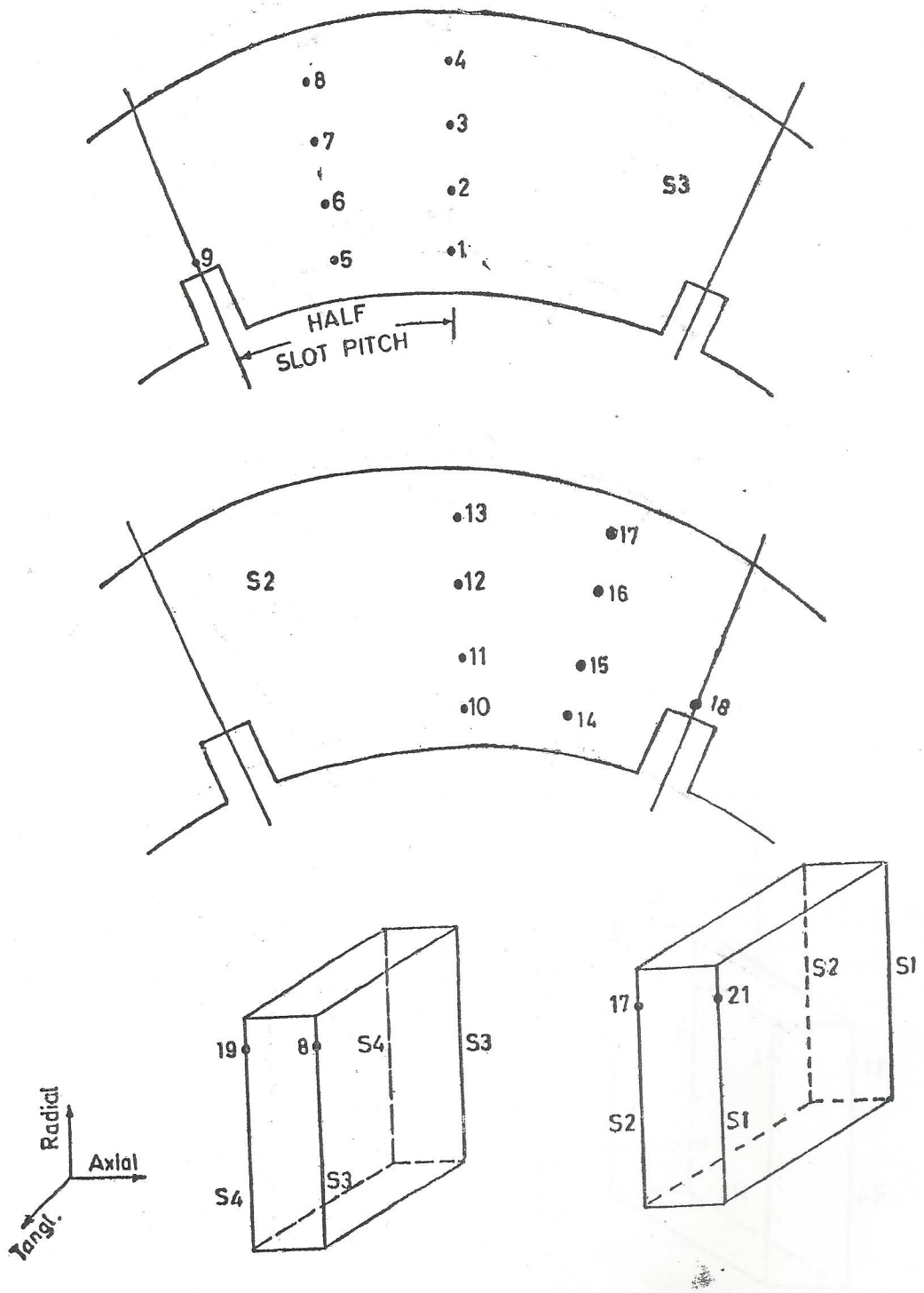

FIG. 3. Location of thermocouples in stator disks.

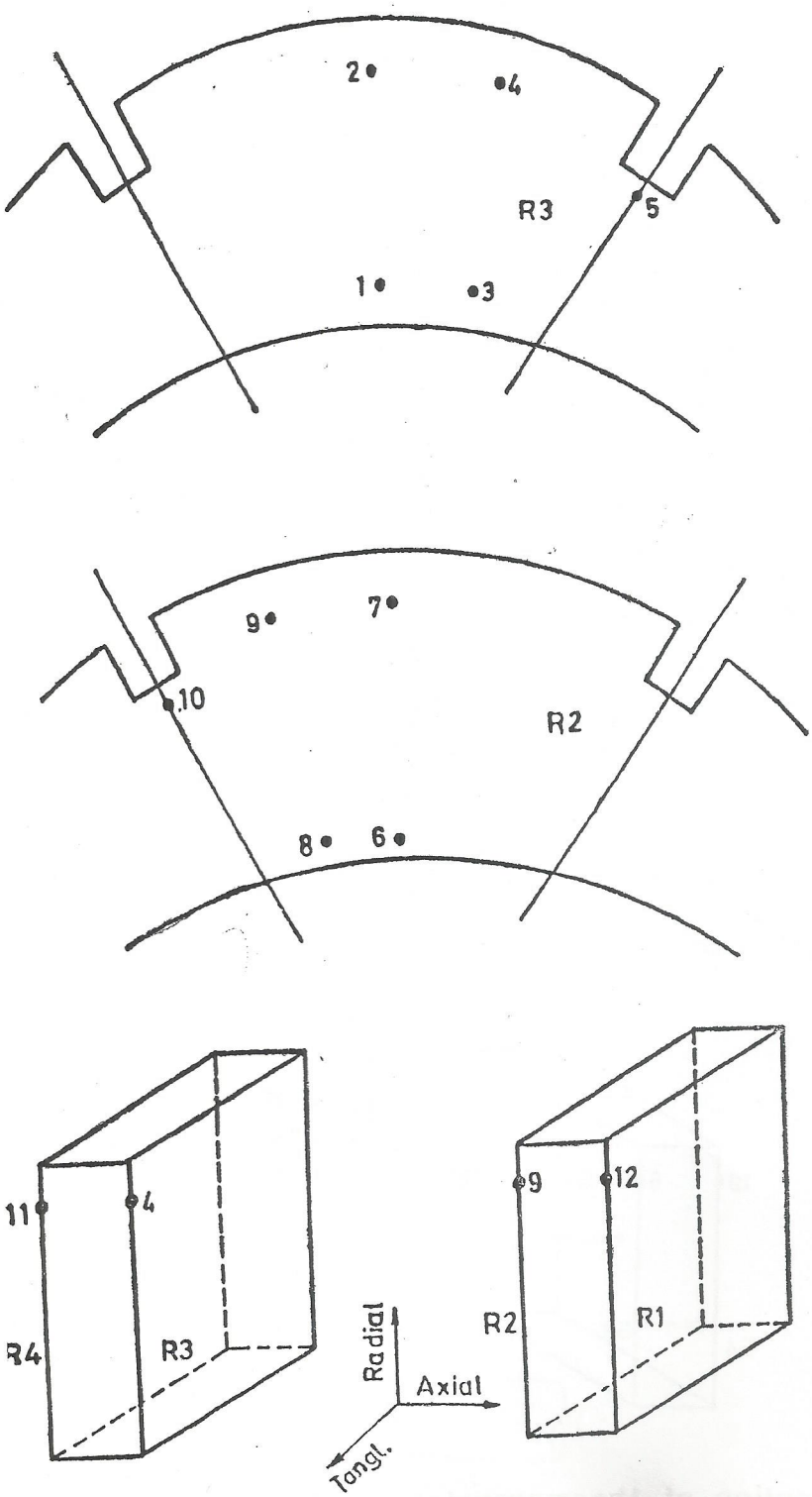

FIG. 4. Location of thermocouples in rotor disks.

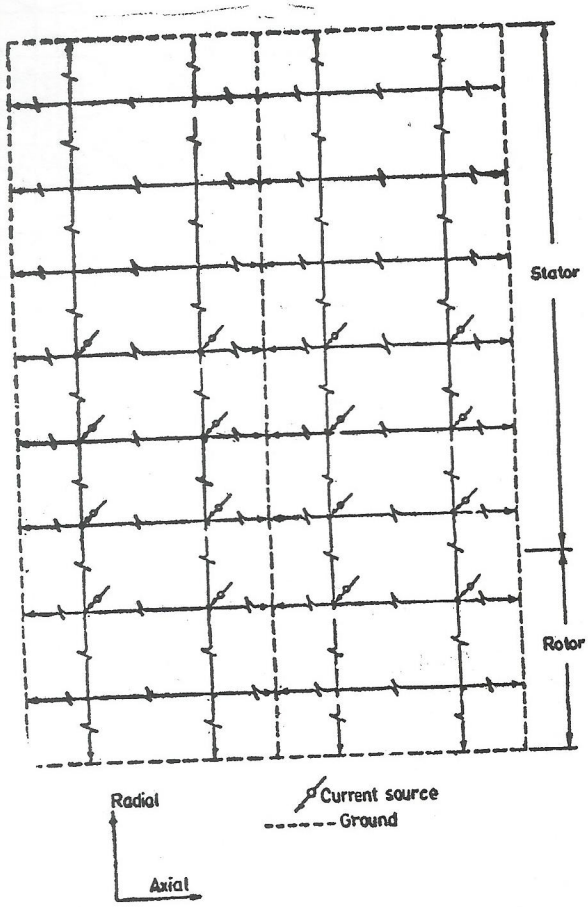

Fig 5. 2-D R-C network for the experimental model

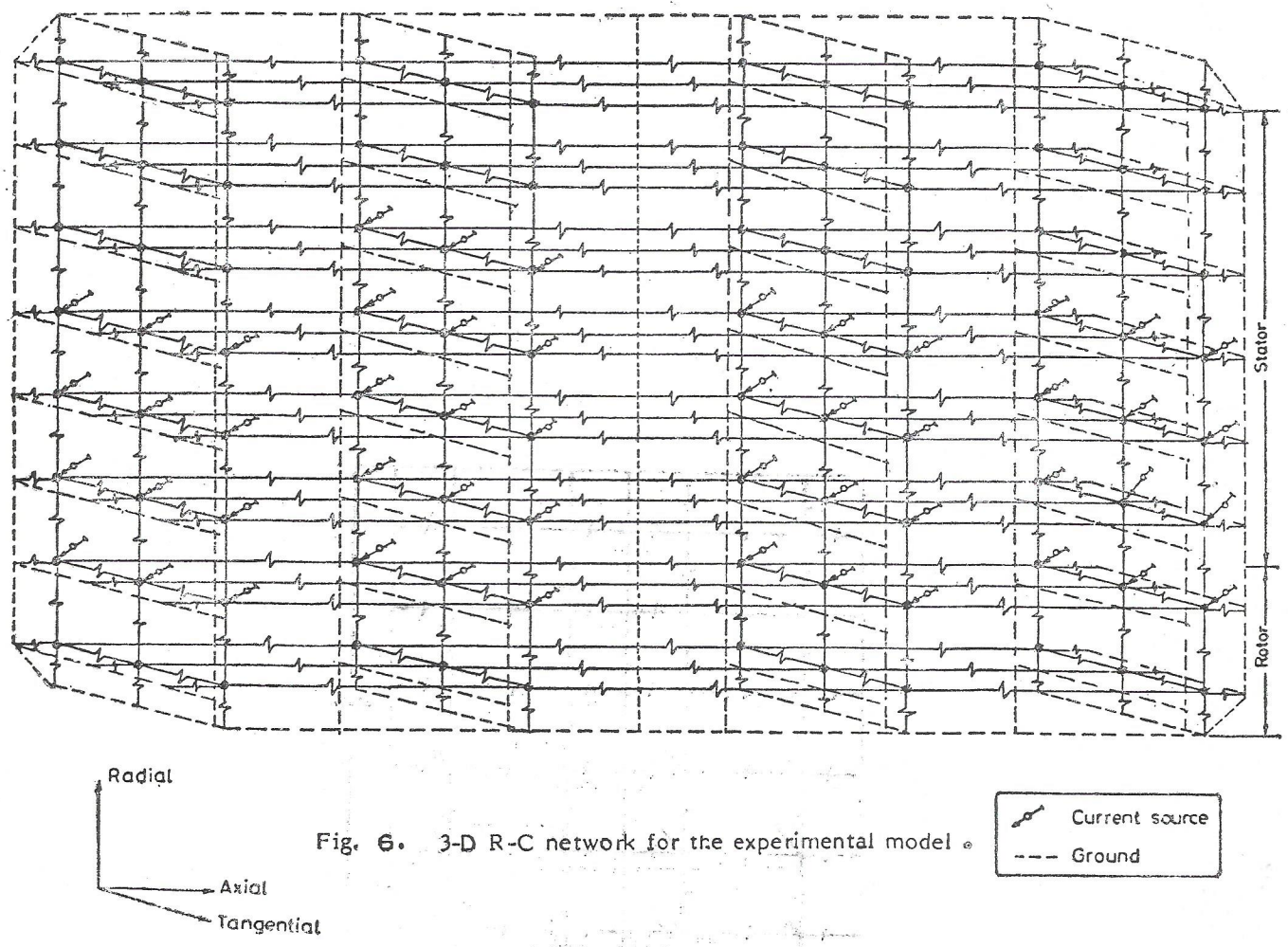

Fig. 6. 3-D R-C network for the experimental model.

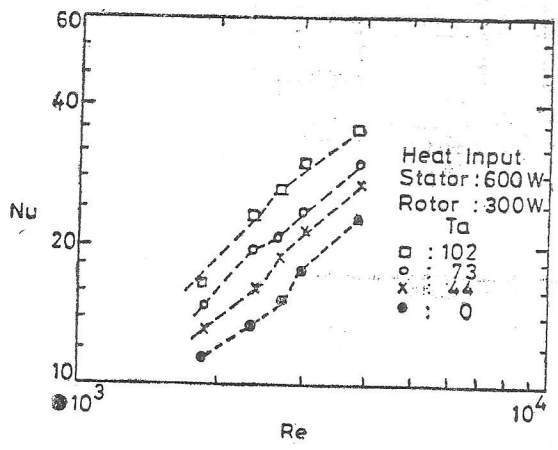

FIG. 7. Nu Vs Re for rotor radial duct at different Ta.

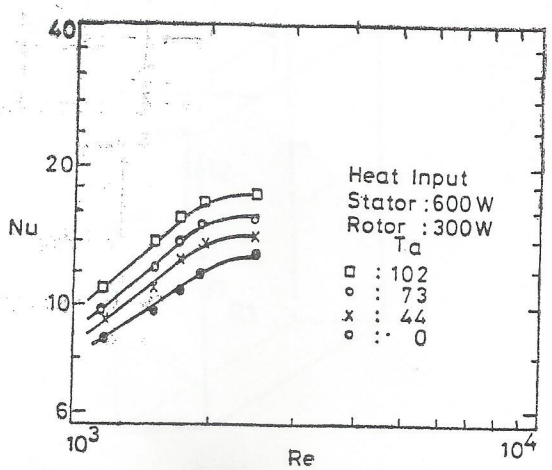

FIG. 8. Nu Vs Re for stator radial duct at different Ta.

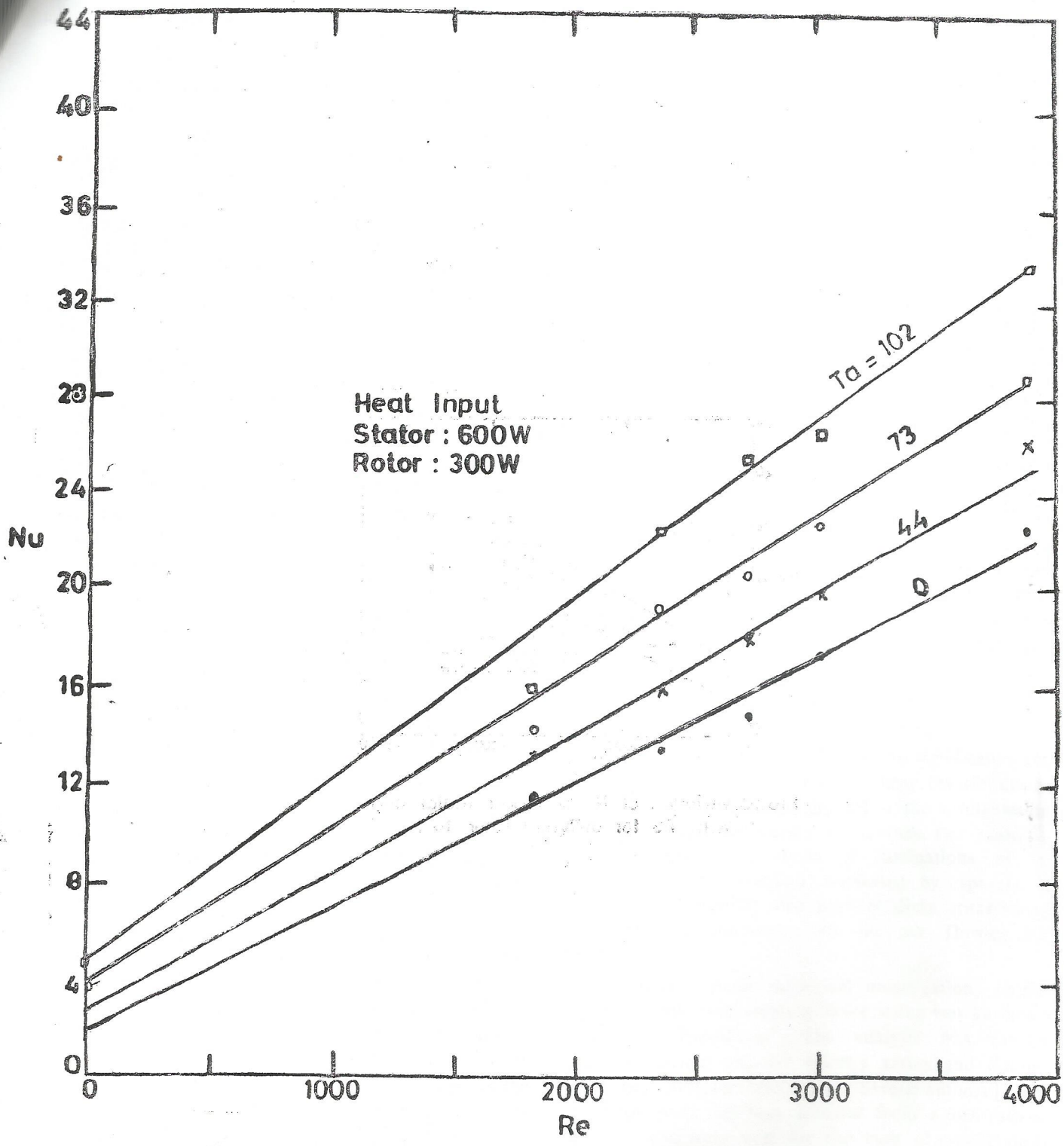

FIG. 9 .Variation of Nu in rotor radial duct with Re for different Ta .

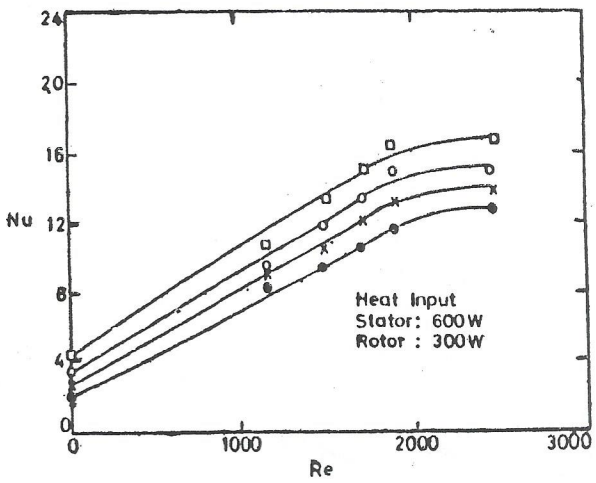

FIG.10. Variation of Nu in stator radial duct with Re for different rotor Ta .